Compound Hot-Dry and Cold-Wet Dynamical Extremes Over the Mediterranean

Paolo De Luca[1,2], Gabriele Messori[2,3], Davide Faranda[4,5], Philip J. Ward[1], and Dim Coumou[1,6]

[1]Department of Water and Climate Risk, Vrije Universiteit Amsterdam, Amsterdam, the Netherlands
[2]Department of Earth Sciences, Uppsala University, Uppsala, Sweden
[3]Department of Meteorology, Stockholm University and Bolin Centre for Climate Research, Stockholm, Sweden
[4]Laboratoire des Sciences du Climat et de l'Environnement, LSCE/IPSL, CEA-CNRS-UVSQ, Université Paris-Saclay, Gif-sur-Yvette, France
[5]London Mathematical Laboratory, London, UK
[6]Royal Netherlands Meteorological Institute (KNMI), De Bilt, the Netherlands

Correspondence: Paolo De Luca (p.deluca@vu.nl)

Abstract. The Mediterranean (MED) basin is a climate change hot-spot that has seen drying and a pronounced increase in heatwaves over the last century. At the same time, it is experiencing increasing heavy precipitation during wintertime cold spells. Understanding and quantifying the risks from compound events over the MED is paramount for present and future disaster risk reduction measures. Here, we apply a novel method to study compound events based on dynamical systems theory and analyse compound temperature and precipitation anomalies over the MED from 1979 to 2018. The dynamical systems analysis measures the strength of the coupling between different atmospheric variables over the MED. Further, we consider compound hot-dry days in summer and cold-wet days in winter. Our results show that these hot-dry and cold-wet compound days are associated with maxima in the temperature-precipitation coupling parameter of the dynamical systems analysis. This indicates that there is a strong interaction between temperature and precipitation during compound events. In summer, we find a significant upward trend in the coupling between temperature and precipitation over 1979-2018, which is likely driven by a stronger coupling during hot and dry days. Thermodynamic processes associated with long-term MED warming can best explain the trend. No such trend is found for wintertime cold-wet compound events. Our findings suggest that long-term warming strengthens the coupling of temperature and precipitation which intensifies hot-dry compound events.

1 Introduction

The Mediterranean (MED) basin is considered a climate change hot-spot and has seen winter drying as well as a pronounced increase in summer heatwaves over recent decades (e.g., Mariotti, 2010; Hoerling et al., 2012; Shohami et al., 2011; Nykjaer, 2009).Summer heatwave trends observed over the historical period are mainly driven by thermodynamic changes, such as increasing temperatures, that exacerbate soil drying and daily maximum temperatures. Drying trends during winter are associated with dynamical changes, likely triggered by increased greenhouse gas and aerosol forcing (Hoerling et al., 2012). However, wintertime heavy precipitation, often in the form of snowfall, has not decreased as rapidly as one may expect (Faranda, 2019).

Many studies have investigated climate change projections over the MED under high greenhouse gases emission scenarios, providing strong evidence for a continuation of the trends witnessed in the historical period, and much warmer and drier conditions by the end of the 21st century (Zappa et al., 2015; Mariotti et al., 2015; Scoccimarro et al., 2016; Hochman et al., 2018; Samuels et al., 2018; Seager et al., 2014; Barcikowska et al., 2020; Goubanova and Li, 2007; Giorgi and Lionello, 2008; Giannakopoulos et al., 2009; Beniston et al., 2007). Such climatic changes imply more severe and frequent summer heatwaves and droughts (Fischer and Schär, 2010; Giorgi and Lionello, 2008; Beniston et al., 2007; Giannakopoulos et al., 2009), but also an increase in precipitation extremes notwithstanding the decline in total precipitation (Scoccimarro et al., 2016; Samuels et al., 2018; Goubanova and Li, 2007; Giannakopoulos et al., 2009). Similar changes are expected during winter, including a reduction of cold spell intensity. For example, Hochman et al. (2020) showed that Cyprus Lows – synoptic low-pressure systems that develop over the Eastern MED and can drive cold spells and heavy precipitation over the Levant – are projected to decrease in frequency and rain-bearing capacity in the future. Changes in atmospheric dynamics, such as an amplified "monsoon-desert mechanism" in summer (Rodwell and Hoskins, 1996; Cherchi et al., 2016; Kim et al., 2019; Wang et al., 2012) or a poleward shift of the tropical belt in winter (Hu and Fu, 2007; Seidel et al., 2008; Peleg et al., 2015; Totz et al., 2018), may play a significant role in enhancing the drying of the MED in future climates.

In recent years, it has become increasingly clear that weather-related impacts often result from the compounding nature of several variables, even if the variables are not extreme when analysed independently. For hazards it is thus important to consider compound, or multi-variate, events (Zscheischler et al., 2018; Leonard et al., 2014), as well as cascading events (de Ruiter et al., 2020). Such compound events can lead to socio-economic damages exceeding those expected if the individual hazards were to occur separately (e.g., de Ruiter et al., 2020; Barriopedro et al., 2011). The MED region is highly vulnerable to compound hot-dry events, such as the co-occurrence of heatwaves and droughts (Zampieri et al., 2017; Li et al., 2009). Wintertime cold-wet events, especially when associated with snowfall, may also result in costly regional impacts (e.g. Hochman et al., 2019; Bisci et al., 2012).

Here, we specifically seek to characterise precipitation - temperature compound events over the MED in terms of the coupling between the large-scale precipitation and temperature fields. This allows us to relate long-term changes in compound events to their underlying physical drivers. We focus on compound hot-dry and cold-wet events during summer (June-July-August, JJA) and winter (December-January-February, DJF), respectively. To diagnose the coupling between atmospheric variables, we apply a method based on dynamical systems theory that reflects the dynamical evolution of the atmosphere (Faranda et al., 2020; De Luca et al., 2020) and is well-suited to diagnosing changes in atmospheric properties (Faranda et al., 2019). The article is structured as follows: Section 2 describes the methods, data and statistical tests. Sections 3-4 present the results. Specifically, Section 3 focuses on the strength of the dynamical coupling during JJA. Section 4 investigates the large-scale patterns of sea-level pressure (SLP), temperature and precipitation observed during the days when the dynamical coupling is high in both JJA and DJF, and relates these to the compound hot-dry and cold-wet events. Finally, Section 5 summarises and discusses our main findings, and outlines future research opportunities.

2 Methods and data

2.1 Dynamical systems metrics

In this study, we use a dynamical systems approach to compute two metrics: θ^{-1} and α. θ^{-1}, which we term *persistence*, is very intuitively a measure of the average residence time of the system around a state of interest. Hence, the higher the value of θ^{-1}, the more likely it is that the preceding and future states of the system will resemble the current state over relatively long timescales (Faranda et al., 2017b; Messori et al., 2017; Hochman et al., 2019). α, which we term *co-recurrence ratio*, is a measure of the dynamical coupling between two variables.

The calculation of the dynamical systems metrics stems from the combination of Poincaré recurrences with extreme value theory (Lucarini et al., 2012; Freitas et al., 2010; Faranda et al., 2020). By *recurrences* we refer to the system being analysed returning arbitrarily close to a previously visited state. Given an atmospheric variable x, we consider a state of interest ζ_x. In our case, this would be an instantaneous configuration of that variable, such as a latitude-longitude temperature map on a given day over the MED. We then consider recurrences to be those states that are close to ζ_x, namely other timesteps at which the selected variable takes a very similar configuration. In order to quantify how close two configurations are to one another, we use the Euclidean distance between latitude-longitude maps. Based on the properties of these recurrences, we can diagnose the dynamical systems persistence θ_x^{-1} of the state ζ_x. θ_x^{-1} measures the average residence time of the system around ζ_x and it has the units of the timestep of the dataset being analysed. If we extend the analysis to two variables, x and y, we can then compute a co-persistence $\theta_{x,y}^{-1}$ based on recurrences around a joint state of interest $\zeta = \{\zeta_x, \zeta_y\}$. In our analysis, the joint state $\zeta = \{\zeta_x, \zeta_y\}$ would simply be the state consisting of the combined instantaneous precipitation and temperature maps.

We further define the co-recurrence ratio α between x and y. Given a state $\zeta = \{\zeta_x, \zeta_y\}$, the co-recurrence ratio $0 \leq \alpha \leq 1$ measures the number of cases where x resembles ζ_x given that y resembles ζ_y, versus the number of cases when only x resembles the relevant reference state. When $\alpha = 0$, there are no co-recurrences of $\zeta = \{\zeta_x, \zeta_y\}$ when we observe a recurrence of ζ_x. When $\alpha = 1$, recurrences of ζ_x are always also co-recurrences of $\zeta = \{\zeta_x, \zeta_y\}$. Hence, α may be interpreted as a measure of the dynamical coupling between x and y. However, α does not indicate causality: indeed, the order of x and y may be exchanged without affecting the value of α. For a schematic depiction of the interpretation of α, and for the mathematical details of the calculations of θ^{-1} and α, we refer the reader to Faranda et al. (2020).

In our analysis, we consider each timestep in our datasets in turn as the state of interest ζ. The final result of our analysis is therefore a value for each indicator and each timestep for the chosen geographical domain. We term the days with $\alpha > 90^{th}$ quantile of the full-year distribution over the whole time-period being analysed *compound dynamical extremes* (CDEs). The two indicators, both in their monovariate and bivariate forms, successfully reflect large-scale features of atmospheric motions, and have recently been applied to a range of different climate variables over different geographical domains (Faranda et al., 2017a, b, 2019, 2020; Messori et al., 2017; Rodrigues et al., 2018; Hochman et al., 2019, 2020; De Luca et al., 2020).

2.2 Data

We use the European Centre for Medium-Range Weather Forecasts' (ECMWF) ERA5 reanalysis over 1979-2018, with a spatial horizontal resolution of 0.25° and a 6-hourly temporal resolution (C3S, 2017). Our MED domain follows the "Full Mediterranean" region described in Giorgi and Lionello (2008). For ERA5, this corresponds to 27.75–48.00 °N, 9.75 °W–39.00 °E. To improve the robustness of our results, we have repeated the bulk of the analysis on ERA-Interim (Dee et al., 2011) and ERA5 10-member ensemble (C3S, 2017) (see Supplementary Material). We use the 6-hourly data to compute daily maximum and minimum 2m temperature (K) and daily total precipitation (mm), from now on termed Tmax, Tmin and P respectively. Hot-dry days are JJA days experiencing positive Tmax and negative P anomalies. Similarly, cold-wet days are DJF days experiencing negative Tmin and positive P anomalies. These are collectively referred to as 'compound events'. We also analyse daily-mean sea-level pressure (SLP, hPa).

2.3 Statistical tests

The statistical significance of the Sen's slopes (Sen, 1968) of the α and θ^{-1} time-series is verified using the Mann-Kendall test (Mann, 1945) from the R package *'modifiedmk_v1.4.0'*. The Sen's slopes provide information about the steepness of the trends. If the Sen's slope is positive (negative) the corresponding trend is increasing (decreasing).

The statistical significance of SLP, Tmax, Tmin and P composite anomalies occurring during CDEs is computed using a one-tailed Mann-Whitney test at the 5% confidence level (Mann and Whitney, 1947). The null hypothesis is that a randomly selected anomaly value during a CDE is equally likely to be less than or greater than a randomly selected value from the days that are not CDEs. The alternative hypothesis is that during JJA (DJF), the SLP and Tmax (Tmin) anomalies observed during CDEs are higher (lower) than the those observed during other days. For P in JJA (DJF), the alternative hypothesis is that anomalies observed during CDEs are lower (higher) than those during other days. To avoid incurring Type I errors (or false positives), we apply the Bonferroni correction to all p-values when considering single-gridpoint data (Bonferroni, 1936). The one-tailed Mann-Whitney test is also applied to the histograms and cumulative distribution functions (CDFs) of the anomaly means occurring during CDEs versus all other days.

3 Temperature-precipitation coupling

During JJA, the co-recurrence ratio (α) between Tmax and P shows a significant upward trend (p-value <0.001) over 1979-2018 (Figures 1a and S1a). This points to an increasingly strong coupling between Tmax and P over time. During DJF, we also observe positive, albeit non-significant α trends for all three reanalysis products (Figure S2). There is a clear correlation between α and summer mean Tmax, as highlighted in Figures 1b and S1b. Indeed, ranking α values by JJA-averages of Tmax results in positive and statistically significant trends (p-values <0.001), comparable in magnitude to those seen in Figures 1a and S1a. Moreover, both a regression analysis and the two-sided Spearman's rank correlation test (Corder and Foreman, 2014) between JJA α values and JJA average Tmax over the MED show a clear association between them (Figure S3). Trends in the

α time-series of both CDE and non-CDE days are upward and statistically significant (Figure S4), pointing to a general shift in the α distribution towards higher values.
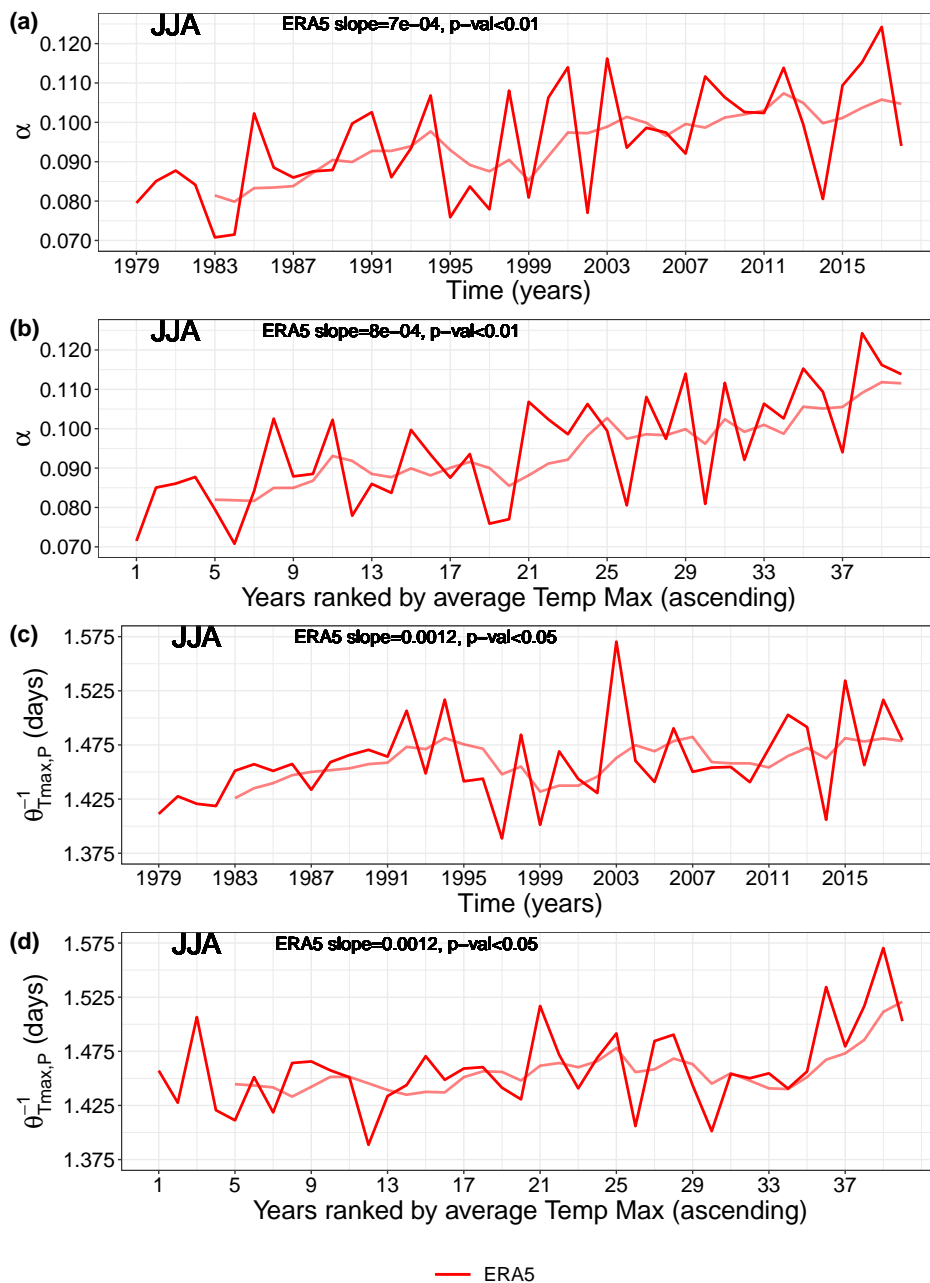
Figure 1. Co-recurrence ratio (α) and local co-persistence $\theta_{Tmax,P}^{-1}$ JJA means for ERA5 during the 1979-2018 period over the Mediterranean. (a) α JJA means; (b) α ranked according to ascending JJA average Tmax; (c) $\theta_{Tmax,P}^{-1}$; and (d) $\theta_{Tmax,P}^{-1}$ ranked according to ascending JJA average Tmax. The thin lines are 5-year moving averages. The Sen's slopes and p-values are also shown. α is computed from Tmax and P.

We next compute the local co-persistence ($\theta^{-1}_{Tmax,P}$) trends during JJA (Figures 1c and S1c) in analogy to Figures 1a and S1a. The significant upward trends (p-value <0.05 for ERA5 and ERA5 ensemble, and p-value <0.01 for ERA-Interim) in $\theta^{-1}_{Tmax,P}$ imply a trend towards longer joint spatial patterns of Tmax and P over the MED within the observational period. Restricting the analysis to hot-dry days highlights similar trends (not shown), pointing towards increasingly long hot-dry events over the region. As for α, changes in co-persistence map directly onto changes in average Tmax in JJA (Figures 1d and S1d). Interestingly, there is a clear peak in $\theta^{-1}_{Tmax,P}$ during summer 2003 for all reanalysis products, coinciding with the extreme 2003 European heatwave (Black et al., 2004; Fischer et al., 2007; Stott et al., 2004). The trends in $\theta^{-1}_{Tmax,P}$ reflect trends in the (univariate) local persistence of Tmax (θ^{-1}_{Tmax}) and P (θ^{-1}_P) (Figures 2 and S5). Trends in θ^{-1}_{Tmax} (Figures 2a and S5a) are stronger than those in θ^{-1}_P (Figures 2b and S5b). This strengthens our interpretation of Tmax as playing a predominant role in setting the observed positive trends in the dynamical indicators.
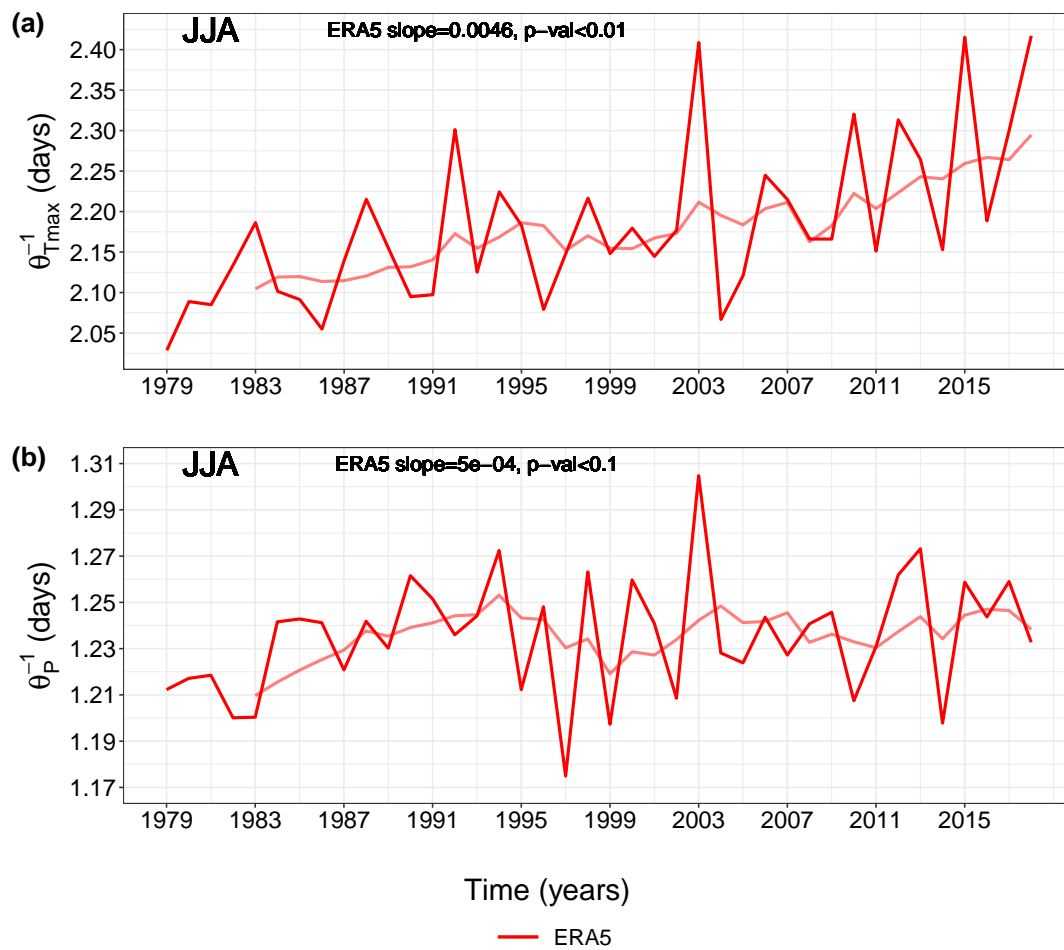
Figure 2. As Figure 1c but for univariate local persistence of (a) Tmax (θ_{Tmax}^{-1}) and (b) P (θ_{P}^{-1}).

4 Compound dynamical extremes (CDEs) linked to compound hot-dry and cold-wet events

4.1 Seasonality of CDEs

130   We next investigate the temporal distribution of CDEs. For α computed on Tmax and P, all three reanalysis products display CDEs clustering in July and August, with a secondary maximum in DJF (Figures 3 and S6). For α computed on Tmin and P, most CDEs occur during DJF, with a secondary maximum in July and August (Figures 3b and S6b). This holds for all reanalyses except ERA-Interim, which shows the highest counts during July and August. Such difference may be linked to ERA-Interim's lower horizontal resolution ($0.75°$), leading to a bias in the quantification of P events. For both variable combinations, the

135   two shoulder seasons (i.e. spring and autumn) display very few CDEs. In Faranda et al. (2017a), the authors hypothesised that during autumn and spring the atmospheric flow sits on a saddle-like point of the dynamics, while winter and summer represent more stable basins of attraction. Assuming that distinct attractors indeed exist for winter and summer, we thus interpret the low CDE counts as the result of the atmospheric flow exploring both summer and winter configurations, resulting in rarer co-recurrences.
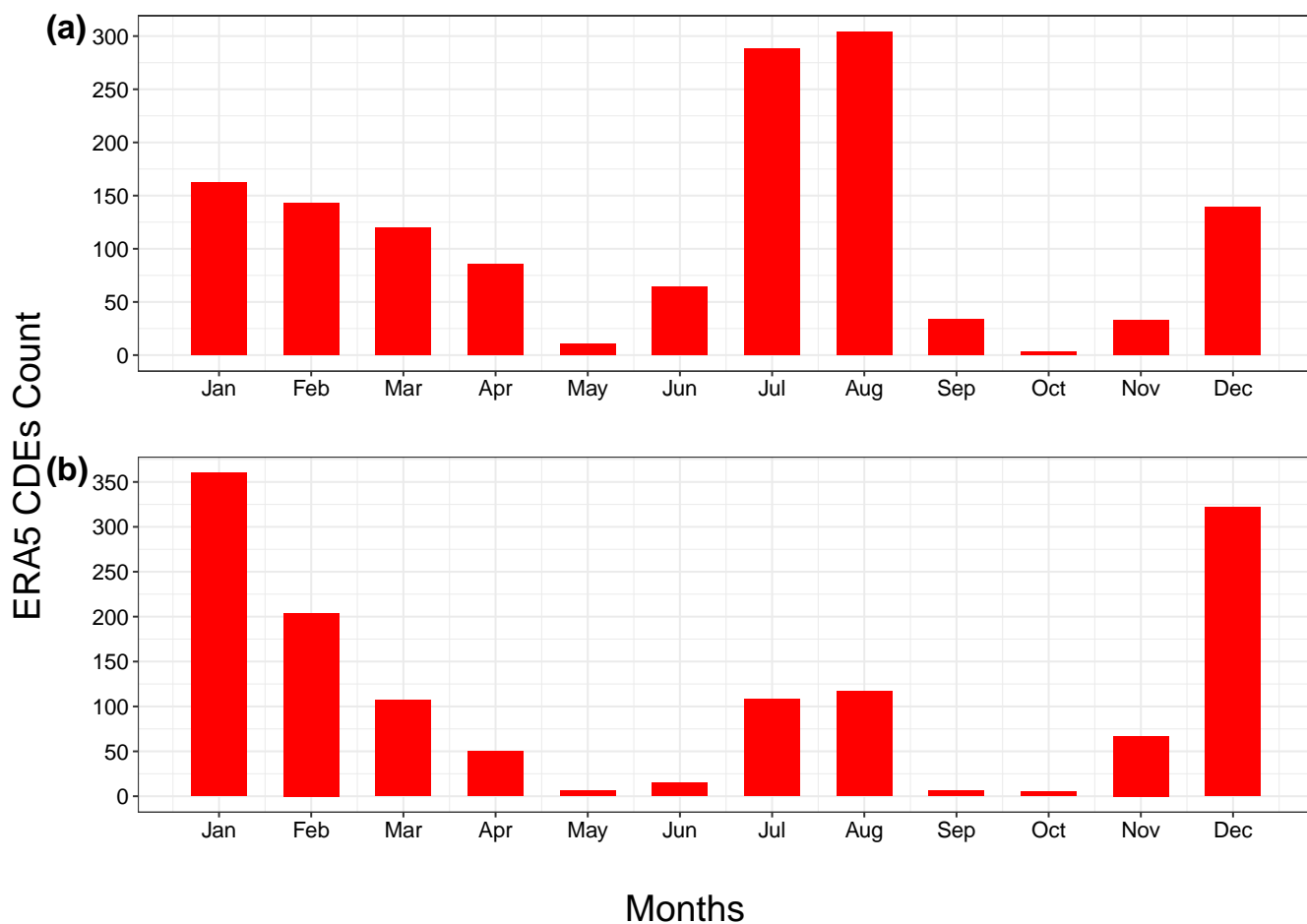
Figure 3. Monthly counts of compound dynamical extremes (CDEs) for ERA 5 during 1979-2018 over the Mediterranean. (a) α computed from Tmax and P; and (b) α computed from Tmin and P. CDEs are defined as α daily observations $> 90^{th}$ quantile of the α distribution for the full dataset.

4.2 Pressure, temperature and precipitation anomalies during CDEs

During JJA, CDEs correspond to statistically significant positive SLP anomalies over the western MED (north-western Africa) and the Anatolia - Black Sea region. These are separated by a band of negative SLP anomalies spanning Italy, part of the Balkans, Crete, the Levant and Northern Egypt (Figures 4a and S7a-b). These SLP anomalies are in turn associated with significant warm Tmax anomalies over most of the MED, with a particularly warm Balkan Peninsula, and a negative anomaly over central northern Africa (Figures 4c and S7c-d). Lastly, we observe weak dry P anomalies over the Black Sea (Figures 4e and S7e-f) and stronger wet P anomalies over the Alps. The latter correspond to statistically significant large-scale P positive anomalies (Figure S8a), rather than convective P anomalies (Figure S8b). This enables us to link these precipitation anomalies to the SLP anomalies discussed above, and in particular to the advection of moist Mediterranean airmasses inland towards the Alpine region. We conclude that JJA CDEs are closely linked to widespread warm Tmax anomalies, but have a weaker footprint on P anomalies, except over the Alps.

In DJF we observe an east-west dipole in SLP over the MED, that favours cold-air advection from northern Europe to the Italian peninsula, the Balkans, and the eastern MED, leading to significant negative Tmin anomalies in these regions. The eastern MED also displays significant positive P anomalies (Figures 4b,d,f and S9). The statistically significant (p-value <0.05) negative SLP anomalies over the eastern MED are reminiscent of the footprint of the Cyprus Lows, which are the main rain-bearing systems over the region (Alpert et al., 2004; Saaroni et al., 2010) (Figures 4b and S9a-b). Cyprus Lows are also associated with the majority of wintertime cold spells over the eastern MED (Hochman et al., 2020), and we indeed find that some of the P anomalies over the eastern MED are snowfall events, particularly over southern Turkey and Lebanon (Figure S10). We thus conclude that CDEs are associated with wintertime cold-wet compound events.
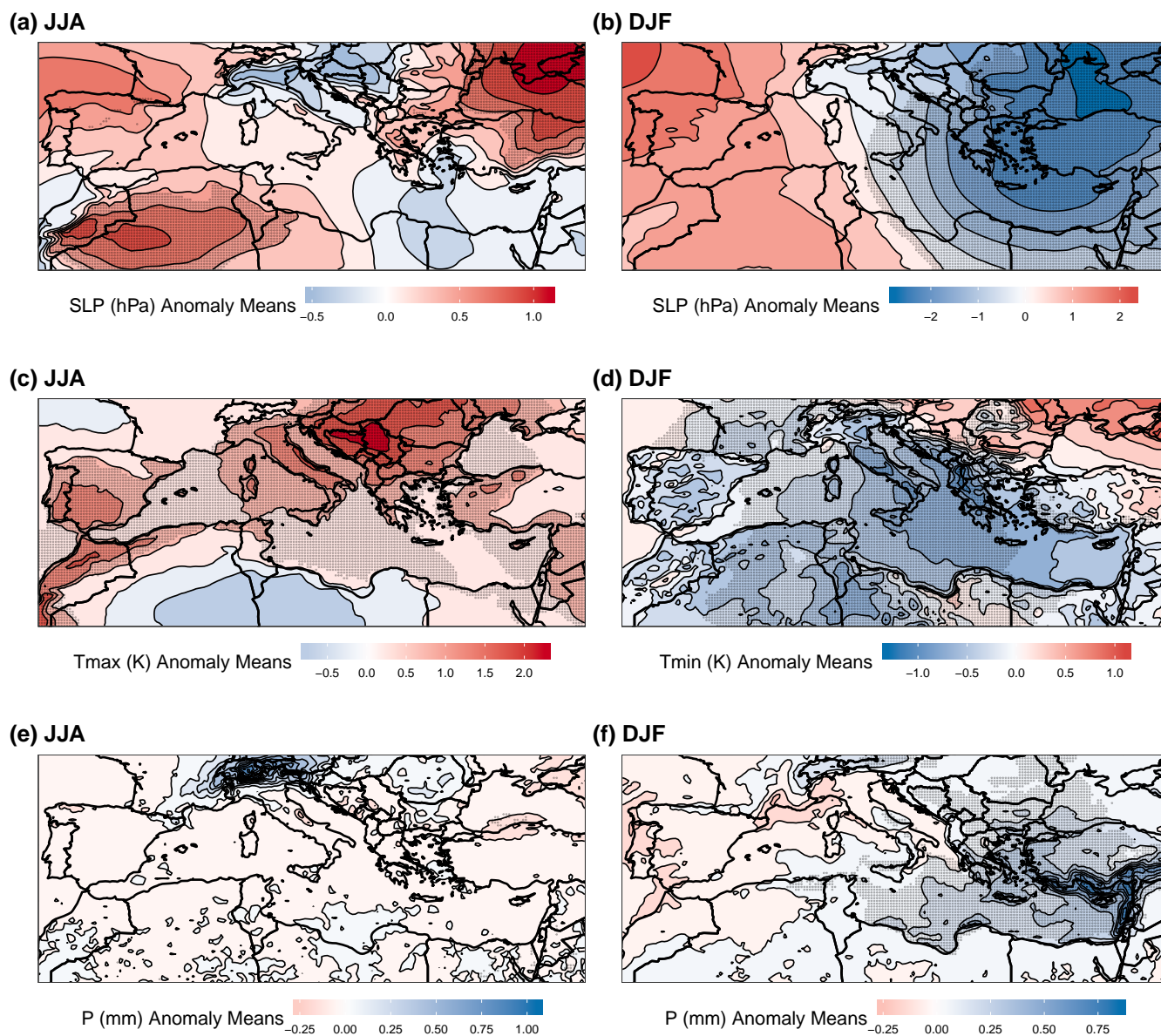
Figure 4. JJA and DJF anomaly means of (a-b) SLP, (c-d) Tmax and Tmin, and (e-f) P during CDE days. The data are from the ERA5 reanalysis during 1979-2018. α for JJA is computed from Tmax and P, whereas for DJF from Tmin and P. Stippling shows statistically significant anomalies (p-value <0.05, Mann-Whitney one-tailed test). The Bonferroni correction is applied to all p-values.

4.3 Distributions of temperature and precipitation anomaly means

160 We next test empirically whether the CDEs highlighted above have a systematic link to compound JJA hot-dry and DJF cold-wet events. During JJA, Tmax and P daily anomaly means, computed for each grid-point during CDEs, are predominantly hot (84%) and dry (77%) respectively (Figure 5a-b). Similar results are also obtained for ERA-Interim and ERA5 ensemble (Figure S11). P anomalies tend to cluster around zero, owing to the overall dry summertime climate of the region, although as noted above they do show a preference for negative (dry) values (Figures 5b and S11b,d). A Mann-Whitney one-tailed test

165 between the anomaly means during CDEs versus all other days in JJA results in statistically significant differences (p-value <0.01) for all reanalysis products for both Tmax and P. This implies that CDEs are significantly hotter and drier than other JJA days.

In DJF, most of the Tmin and P anomaly means are cold (77%) and wet (66%) respectively for ERA5 (Figure 5c-d) and the other reanalysis products (Figure S12). The CDEs therefore present a somewhat mirror image of the preferred anomalies seen

170 in both JJA and DJF. Again, a Mann-Whitney one-tailed test between anomaly means during CDEs and all other DJF days highlights statistically significant (p-value <0.01) differences for all reanalysis products' Tmin and P. This implies that CDEs are significantly colder and wetter than all other DJF days.
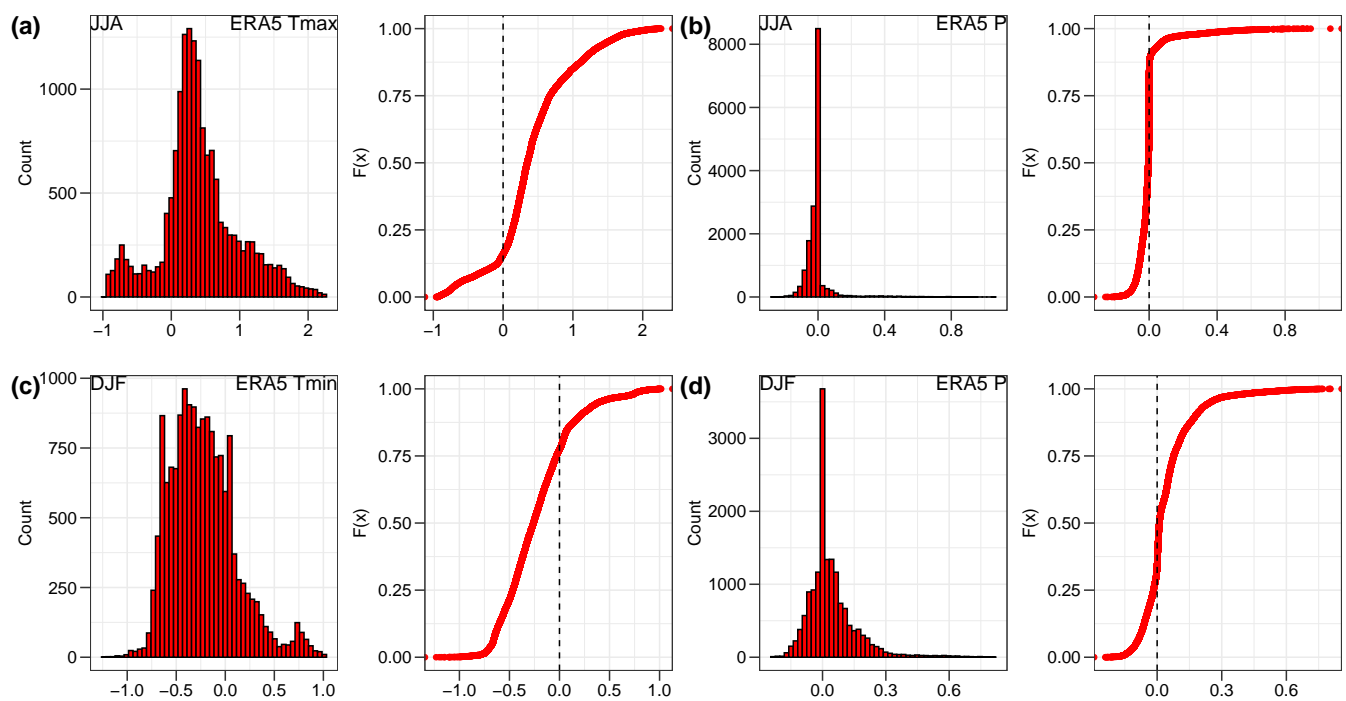
Figure 5. Histograms and cumulative distribution functions (CDFs) of anomaly means of (a) Tmax, (b) P during JJA CDEs, and (c) Tmin, (d) P during DJF CDEs. The data are the same as in Figure 4c-f. The distributions are statistically different from those of all other JJA and DJF days, respectively (p-value <0.01, Mann-Whitney one-tailed test).

4.4 Spatial patterns of compound hot-dry and cold-wet events

We next complement the statistical information provided by the histograms and CDFs with spatial distributions of percentage
175   (%) match between compound events and CDEs. Across the MED, a high fraction of compound hot-dry events during JJA
coincide with CDEs. Values locally exceed 70%, meaning that >70% of all JJA compound hot-dry events occur during CDEs
(Figures 6a and S13). The highest percentages occur along a belt stretching from southern Spain to Italy, the central-eastern
MED and the Balkans. During DJF, the % match between compound cold-wet events and CDEs is lower than that seen for hot-
dry JJA events (<50%) (Figures 6b and S14). The highest % of compound events occurs over the eastern MED sea, between
180   the coastlines of Libya, Egypt, Greece and Turkey.

(a)

ERA5 JJA Hot–Dry %

10 20 30 40 50 60 70

(b)

ERA5 DJF Cold–Wet %

10   20   30
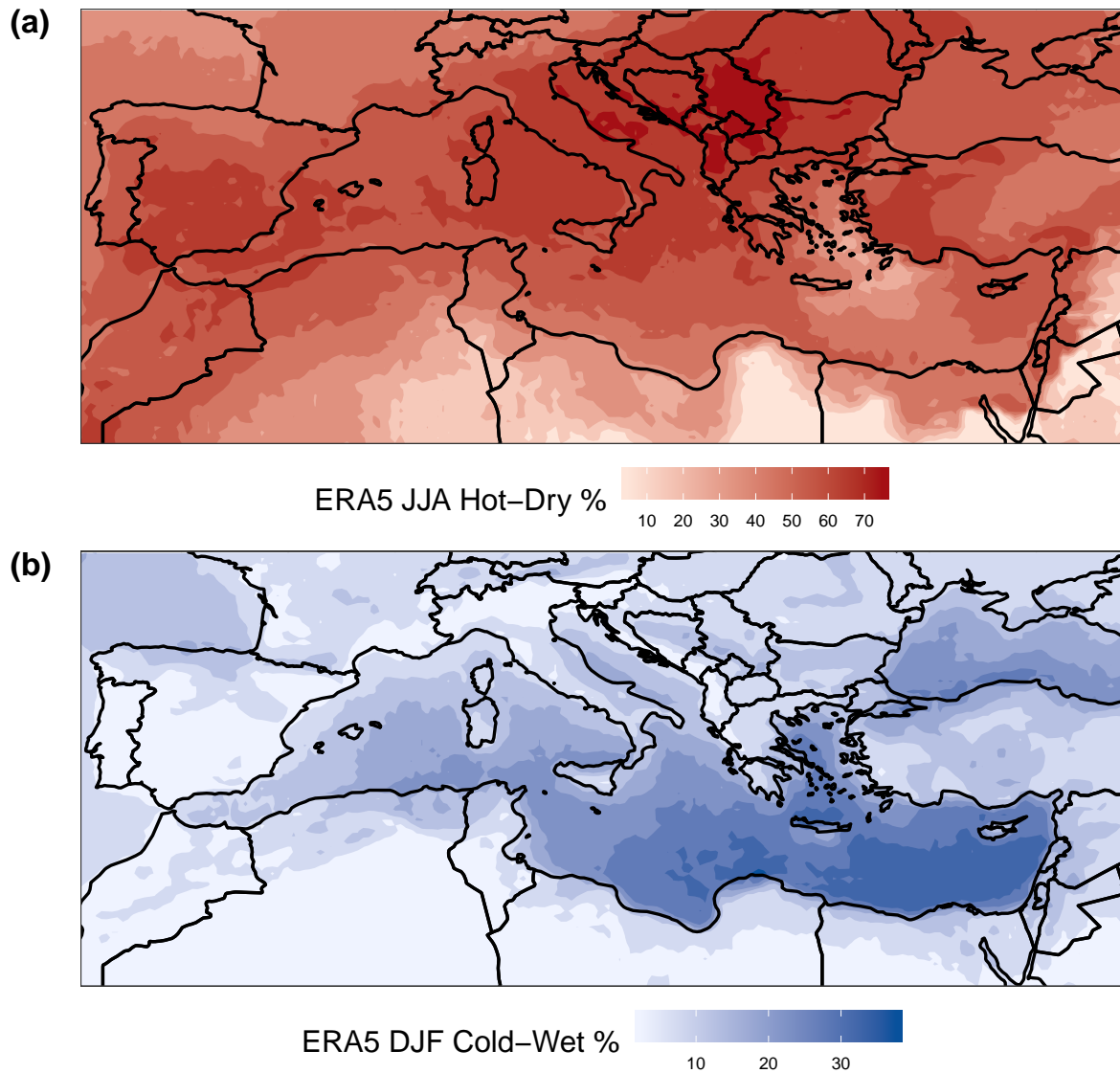
Figure 6. Percentage (%) of compound (a) JJA hot-dry and (b) DJF cold-wet events occurring during CDEs. The data are from the ERA5 reanalysis during 1979-2018.

5 Discussion and conclusions

In this paper, we analysed compound hot-dry (cold-wet) events during JJA (DJF) over the MED through the lens of dynamical systems theory. We specifically computed a measure of coupling (α) between daily maximum temperature (Tmax) and total precipitation (P) during JJA and and daily minimum temperature (Tmin) and P during DJF. We then identified days when the two variables are strongly coupled ($\alpha > 90^{th}$ percentile of its full distribution) and termed them compound dynamical extremes (CDEs). We further computed a dynamical systems measure of the persistence of large-scale configurations in the above variables (θ^{-1}), considering them both individually and in pairs.

During JJA, α and $\theta^{-1}_{Tmax,P}$, namely the persistence of joint large-scale configurations of Tmax and P, both display significant upward trends. An upward persistence trend is also found if we focus specifically on hot-dry days. We propose these trends are driven by surface warming over the MED. A possible physical process driving increasing coupling with increasing temperature is soil drying, although we didn't investigate this in detail here. Specifically, the increasingly warm summer temperatures may lead to significantly lower soil-moisture content, triggering a feedback mechanism that favours persistent hot-dry conditions. Consistently with this, we found that CDEs computed from Tmax and P cluster during July and August, whereas CDEs computed from Tmin and P cluster during DJF. During CDE days, synoptic patterns in JJA show significant positive SLP and hot Tmax anomalies over large parts of the MED, and dry but weaker anomalies for P. The latter is somewhat unsurprising, as the low climatological summertime precipitation over the region effectively prevents the occurrence of large negative precipitation anomalies. In DJF CDEs are associated with significant negative SLP anomalies and cold-wet anomalies centred over the Eastern Mediterranean. The distributions of anomalies occurring during CDEs are significantly different (p-value <0.01) from the ones recorded during all other days. Lastly, we found that CDEs correspond to a heightened frequency of positive Tmax anomalies during JJA and a heightened frequency of negative Tmin and positive P anomalies during DJF over large parts of the MED. The percentages of cold-wet days during DJF matching CDE days are, however, lower than those found during summer for hot-dry days.

The findings that summertime Tmax and P have become more strongly coupled over the last 40 years, and that the persistence of hot-dry days has increased, are in agreement with Zscheischler and Seneviratne (2017). The latter showed that land-atmosphere feedbacks in a warmer world may lead to an increase in hot-dry summers larger than what may be expected by analysing the projected temperature and precipitation changes as single variables. Assuming a continued increase in future temperatures, we may therefore expect a continued increase in JJA α and θ^{-1} trends, leading to a higher frequency of compound JJA hot-dry events.

The analysis of DJF CDEs, matching cold-wet events, points to very different dynamics. Here, the largest anomalies in SLP, Tmin and P are found over the Eastern Mediterranean, and are reminiscent of the footprint of Cyprus Lows. These are wintertime synoptic systems that play a predominant role in driving cold spells and heavy precipitation events over the Levant (Hochman et al., 2019, e.g.). Our findings show no significant increase in α values during DJF, in accordance with studies

suggesting a decrease in Cyprus Lows frequency, persistence and associated precipitation over the eastern MED (Hochman et al., 2020, 2018; Peleg et al., 2015).

215   Our findings highlight a close connection between CDEs, computed from dynamical systems coupling, and compound hot-dry and cold-wet events over the MED. It is of particular interest that α distinguishes between JJA hot-dry and DJF cold-wet compound events. Based on our results we thus believe that the co-recurrence ratio (α) may be fruitfully used in forthcoming studies to elucidate potential future seasonal climate changes over the MED. We envisage making use of CMIP6 data under different Shared Socioeconomic Pathways (SSPs) up to 2100 (O'Neill et al., 2016) and abrupt climate change simulations (e.g.
220   4xCO2) (Eyring et al., 2016). These investigations may also shed some light on possible tipping points over the MED (Lenton et al., 2008; Lenton, 2011).

Author contributions. PDL designed the study, performed the analyses and created the figures. GM, DF and DC contributed to the methods and study design. PDL and GM wrote the first manuscript draft. All the authors contributed to the writing.

Competing interests. The authors declare that they have no conflicts of interest.

225 *Acknowledgements.* This paper is TiPES contribution #15: This project has received funding from the European Union's Horizon 2020 research and innovation programme under grant agreement No 820970. PDL was also supported by an E-COST STSM (DAMOCLES, Action CA17109). GM was partly supported by the Swedish Research Council Vetenskapsrådet under grant agreement No. 2016-03724. PJW was pupported by a VIDI grant from the Dutch Research Council (NWO, grant nr: 016.161.324).

References

230 Alpert, P., Osetinsky, I., Ziv, B., and Shafir, H.: Semi-objective classification for daily synoptic systems: application to the eastern Mediter-
ranean climate change, International Journal of Climatology, 24, 1001–1011, https://doi.org/10.1002/joc.1036, https://rmets.onlinelibrary.
wiley.com/doi/abs/10.1002/joc.1036, 2004.

Barcikowska, M. J., Kapnick, S. B., Krishnamurty, L., Russo, S., Cherchi, A., and Folland, C. K.: Changes in the future summer Mediter-
ranean climate: contribution of teleconnections and local factors, Earth System Dynamics, 11, 161–181, https://doi.org/10.5194/esd-11-
235   161-2020, https://www.earth-syst-dynam.net/11/161/2020/, 2020.

Barriopedro, D., Fischer, E. M., Luterbacher, J., Trigo, R. M., and García-Herrera, R.: The Hot Summer of 2010: Redrawing the Temperature
Record Map of Europe, Science, 332, 220 LP – 224, https://doi.org/10.1126/science.1201224, 2011.

Beniston, M., Stephenson, D. B., Christensen, O. B., Ferro, C. A. T., Frei, C., Goyette, S., Halsnaes, K., Holt, T., Jylhä, K., Koffi, B.,
Palutikof, J., Schöll, R., Semmler, T., and Woth, K.: Future extreme events in European climate: an exploration of regional climate model
240   projections, Climatic Change, 81, 71–95, https://doi.org/10.1007/s10584-006-9226-z, https://doi.org/10.1007/s10584-006-9226-z, 2007.

Bisci, C., Fazzini, M., Beltrando, G., Cardillo, A., and Romeo, V.: The February 2012 exceptional snowfall along the Adriatic side of Cen-
tral Italy, Meteorologische Zeitschrift, 21, 503–508, https://doi.org/10.1127/0941-2948/2012/0536, http://dx.doi.org/10.1127/0941-2948/
2012/0536, 2012.

Black, E., Blackburn, M., Harrison, G., Hoskins, B., and Methven, J.: Factors contributing to the summer 2003 European heatwave, Weather,
245   59, 217–223, https://doi.org/10.1256/wea.74.04, https://doi.org/10.1256/wea.74.04, 2004.

Bonferroni, C.: Teoria statistica delle classi e calcolo delle probabilita, Pubblicazioni del R Istituto Superiore di Scienze Economiche e
Commericiali di Firenze, 8, 3–62, 1936.

C3S: ERA5: Fifth generation of ECMWF atmospheric reanalyses of the global climate, https://cds.climate.copernicus.eu/cdsapp{#}!/home,
2017.

250 Cherchi, A., Annamalai, H., Masina, S., Navarra, A., and Alessandri, A.: Twenty-first century projected summer mean climate in the Mediter-
ranean interpreted through the monsoon-desert mechanism, Climate Dynamics, 47, 2361–2371, https://doi.org/10.1007/s00382-015-2968-
4, https://doi.org/10.1007/s00382-015-2968-4, 2016.

Corder, G. W. and Foreman, D. I.: Nonparametric Statistics: A Step-by-Step Approach, Wiley, 2014.

De Luca, P., Messori, G., Pons, F., and Faranda, D.: Dynamical Systems Theory Sheds New Light on Compound Climate Extremes in
255   Europe and Eastern North America, Quarterly Journal of the Royal Meteorological Society, https://doi.org/10.1002/qj.3757, https://doi.
org/10.1002/qj.3757, 2020.

de Ruiter, M. C., Couasnon, A., van den Homberg, M. J. C., Daniell, J. E., Gill, J. C., and Ward, P. J.: Why We Can No Longer Ignore
Consecutive Disasters, Earth's Future, 8, e2019EF001425, https://doi.org/10.1029/2019EF001425, https://agupubs.onlinelibrary.wiley.
com/doi/abs/10.1029/2019EF001425, e2019EF001425 2019EF001425, 2020.

260 Dee, D. P., Uppala, S. M., Simmons, A. J., Berrisford, P., Poli, P., Kobayashi, S., Andrae, U., Balmaseda, M. A., Balsamo, G., Bauer,
P., Bechtold, P., Beljaars, A. C. M., van de Berg, L., Bidlot, J., Bormann, N., Delsol, C., Dragani, R., Fuentes, M., Geer, A. J., Haim-
berger, L., Healy, S. B., Hersbach, H., Hólm, E. V., Isaksen, L., Kållberg, P., Köhler, M., Matricardi, M., McNally, A. P., Monge-Sanz,
B. M., Morcrette, J.-J., Park, B.-K., Peubey, C., de Rosnay, P., Tavolato, C., Thépaut, J.-N., and Vitart, F.: The ERA-Interim reanalysis:
configuration and performance of the data assimilation system, Quarterly Journal of the Royal Meteorological Society, 137, 553–597,
265   https://doi.org/10.1002/qj.828, http://dx.doi.org/10.1002/qj.828, 2011.

Eyring, V., Bony, S., Meehl, G. A., Senior, C. A., Stevens, B., Stouffer, R. J., and Taylor, K. E.: Overview of the Coupled Model Intercomparison Project Phase 6 (CMIP6) experimental design and organization, Geoscientific Model Development, 9, 1937–1958, https://doi.org/10.5194/gmd-9-1937-2016, https://www.geosci-model-dev.net/9/1937/2016/, 2016.

Faranda, D.: An attempt to explain recent trends in European snowfall extremes, Weather and Climate Dynamics Discussions, 2019, 1–20,
270   https://doi.org/10.5194/wcd-2019-15, http://www.weather-clim-dynam-discuss.net/wcd-2019-15/, 2019.

Faranda, D., Messori, G., Alvarez-Castro, M. C., and Yiou, P.: Dynamical properties and extremes of Northern Hemisphere climate fields over the past 60 years, Nonlin. Processes Geophys., 24, 713–725, https://doi.org/10.5194/npg-24-713-2017, https://www.nonlin-processes-geophys.net/24/713/2017/https://www.nonlin-processes-geophys.net/24/713/2017/npg-24-713-2017.pdf, 2017a.

Faranda, D., Messori, G., and Yiou, P.: Dynamical proxies of North Atlantic predictability and extremes, Scientific Reports, 7, 41 278, 2017b.

275 Faranda, D., Alvarez-Castro, M. C., Messori, G., Rodrigues, D., and Yiou, P.: The hammam effect or how a warm ocean enhances large scale atmospheric predictability, Nature communications, 10, 1–7, 2019.

Faranda, D., Messori, G., and Yiou, P.: Diagnosing concurrent drivers of weather extremes: application to warm and cold days in North America, Climate Dynamics, https://doi.org/10.1007/s00382-019-05106-3, https://doi.org/10.1007/s00382-019-05106-3, 2020.

Fischer, E. M. and Schär, C.: Consistent geographical patterns of changes in high-impact European heatwaves, Nature Geoscience, 3, 398,
280   2010.

Fischer, E. M., Seneviratne, S. I., Vidale, P. L., Lüthi, D., and Schär, C.: Soil Moisture–Atmosphere Interactions during the 2003 European Summer Heat Wave, Journal of Climate, 20, 5081–5099, https://doi.org/10.1175/JCLI4288.1, https://doi.org/10.1175/JCLI4288.1, 2007.

Freitas, A. C. M., Freitas, J. M., and Todd, M.: Hitting time statistics and extreme value theory, Probability Theory and Related Fields, 147, 675–710, https://doi.org/10.1007/s00440-009-0221-y, https://doi.org/10.1007/s00440-009-0221-y, 2010.

285 Giannakopoulos, C., Sager, P. L., Bindi, M., Moriondo, M., Kostopoulou, E., and Goodess, C.: Climatic changes and associated impacts in the Mediterranean resulting from a 2 °C global warming, Global and Planetary Change, 68, 209 – 224, https://doi.org/https://doi.org/10.1016/j.gloplacha.2009.06.001, http://www.sciencedirect.com/science/article/pii/S0921818109001131, 2009.

Giorgi, F. and Lionello, P.: Climate change projections for the Mediterranean region, Global and Planetary Change, 63, 90 – 104,
290   https://doi.org/https://doi.org/10.1016/j.gloplacha.2007.09.005, http://www.sciencedirect.com/science/article/pii/S0921818107001750, mediterranean climate: trends, variability and change, 2008.

Goubanova, K. and Li, L.: Extremes in temperature and precipitation around the Mediterranean basin in an ensemble of future climate scenario simulations, Global and Planetary Change, 57, 27 – 42, https://doi.org/https://doi.org/10.1016/j.gloplacha.2006.11.012, http://www.sciencedirect.com/science/article/pii/S092181810600275X, extreme Climatic Events, 2007.

295 Hochman, A., Harpaz, T., Saaroni, H., and Alpert, P.: The seasons' length in 21st century CMIP5 projections over the eastern Mediterranean, International Journal of Climatology, 38, 2627–2637, https://doi.org/10.1002/joc.5448, 2018.

Hochman, A., Alpert, P., Harpaz, T., Saaroni, H., and Messori, G.: A new dynamical systems perspective on atmospheric predictability: Eastern Mediterranean weather regimes as a case study, Science Advances, 5, eaau0936, https://doi.org/10.1126/sciadv.aau0936, http://advances.sciencemag.org/content/5/6/eaau0936.abstract, 2019.

300 Hochman, A., Alpert, P., Kunin, P., Rostkier-Edelstein, D., Harpaz, T., Saaroni, H., and Messori, G.: The dynamics of cyclones in the twentyfirst century: the Eastern Mediterranean as an example, Climate Dynamics, 54, 561–574, https://doi.org/10.1007/s00382-019-05017-3, https://doi.org/10.1007/s00382-019-05017-3, 2020.

Hoerling, M., Eischeid, J., Perlwitz, J., Quan, X., Zhang, T., and Pegion, P.: On the Increased Frequency of Mediterranean Drought, Journal of Climate, 25, 2146–2161, https://doi.org/10.1175/JCLI-D-11-00296.1, https://doi.org/10.1175/JCLI-D-11-00296.1, 2012.

305 Hu, Y. and Fu, Q.: Observed poleward expansion of the Hadley circulation since 1979, Atmospheric Chemistry and Physics, 7, 5229–5236, https://doi.org/10.5194/acp-7-5229-2007, https://www.atmos-chem-phys.net/7/5229/2007/, 2007.

Kim, G.-U., Seo, K.-H., and Chen, D.: Climate change over the Mediterranean and current destruction of marine ecosystem, Scientific Reports, 9, 18 813, https://doi.org/10.1038/s41598-019-55303-7, https://doi.org/10.1038/s41598-019-55303-7, 2019.

Lenton, T. M.: Early warning of climate tipping points, Nature Climate Change, 1, 201–209, https://doi.org/10.1038/nclimate1143, https://doi.org/10.1038/nclimate1143, 2011.

310 Lenton, T. M., Held, H., Kriegler, E., Hall, J. W., Lucht, W., Rahmstorf, S., and Schellnhuber, H. J.: Tipping elements in the Earth's climate system, Proceedings of the National Academy of Sciences, 105, 1786–1793, https://doi.org/10.1073/pnas.0705414105, https://www.pnas.org/content/105/6/1786, 2008.

Leonard, M., Westra, S., Phatak, A., Lambert, M., van den Hurk, B., McInnes, K., Risbey, J., Schuster, S., Jakob, D., and Stafford-Smith,
315 M.: A compound event framework for understanding extreme impacts, Wiley Interdisciplinary Reviews: Climate Change, 5, 113–128, https://doi.org/10.1002/wcc.252, 2014.

Li, Y., Ye, W., Wang, M., and Yan, X.: Climate change and drought: a risk assessment of crop-yield impacts , Climate Research, 39, 31–46, https://www.int-res.com/abstracts/cr/v39/n1/p31-46, 2009.

Lucarini, V., Faranda, D., and Wouters, J.: Universal Behaviour of Extreme Value Statistics for Selected Observables of Dynamical Systems,
320 Journal of Statistical Physics, 147, 63–73, https://doi.org/10.1007/s10955-012-0468-z, https://doi.org/10.1007/s10955-012-0468-z, 2012.

Mann, H. B.: Nonparametric Tests Against Trend, Econometrica, 13, 245–259, http://www.jstor.org/stable/1907187, 1945.

Mann, H. B. and Whitney, D. R.: On a test of whether one of two random variables is stochastically larger than the other, The annals of mathematical statistics, pp. 50–60, 1947.

Mariotti, A.: Recent Changes in the Mediterranean Water Cycle: A Pathway toward Long-Term Regional Hydroclimatic Change?, Journal
325 of Climate, 23, 1513–1525, https://doi.org/10.1175/2009JCLI3251.1, https://doi.org/10.1175/2009JCLI3251.1, 2010.

Mariotti, A., Pan, Y., Zeng, N., and Alessandri, A.: Long-term climate change in the Mediterranean region in the midst of decadal variability, Climate Dynamics, 44, 1437–1456, https://doi.org/10.1007/s00382-015-2487-3, https://doi.org/10.1007/s00382-015-2487-3, 2015.

Messori, G., Caballero, R., and Faranda, D.: A dynamical systems approach to studying midlatitude weather extremes, Geophysical Research Letters, 44, 3346–3354, https://doi.org/10.1002/2017GL072879, https://doi.org/10.1002/2017GL072879, 2017.

330 Nykjaer, L.: Mediterranean Sea surface warming 1985–2006, Climate Research, 39, 11–17, https://doi.org/https://doi.org/10.3354/cr00794, 2009.

O'Neill, B. C., Tebaldi, C., van Vuuren, D. P., Eyring, V., Friedlingstein, P., Hurtt, G., Knutti, R., Kriegler, E., Lamarque, J.-F., Lowe, J., Meehl, G. A., Moss, R., Riahi, K., and Sanderson, B. M.: The Scenario Model Intercomparison Project (ScenarioMIP) for CMIP6, Geoscientific Model Development, 9, 3461–3482, https://doi.org/10.5194/gmd-9-3461-2016, https://www.geosci-model-dev.net/9/3461/
335 2016/, 2016.

Peleg, N., Bartov, M., and Morin, E.: CMIP5-predicted climate shifts over the East Mediterranean: implications for the transition region between Mediterranean and semi-arid climates, International Journal of Climatology, 35, 2144–2153, https://doi.org/10.1002/joc.4114, https://rmets.onlinelibrary.wiley.com/doi/abs/10.1002/joc.4114, 2015.

Rodrigues, D., Alvarez-Castro, M. C., Messori, G., Yiou, P., Robin, Y., and Faranda, D.: Dynamical Properties of the North Atlantic
340   Atmospheric Circulation in the Past 150 Years in CMIP5 Models and the 20CRv2c Reanalysis, Journal of Climate, 31, 6097–6111,
       https://doi.org/10.1175/JCLI-D-17-0176.1, https://doi.org/10.1175/JCLI-D-17-0176.1, 2018.

Rodwell, M. J. and Hoskins, B. J.: Monsoons and the dynamics of deserts, Quarterly Journal of the Royal Meteorological Society, 122,
       1385–1404, https://doi.org/10.1002/qj.49712253408, 1996.

Saaroni, H., Halfon, N., Ziv, B., Alpert, P., and Kutiel, H.: Links between the rainfall regime in Israel and location and intensity of Cyprus
345   lows, International Journal of Climatology, 30, 1014–1025, https://doi.org/10.1002/joc.1912, https://rmets.onlinelibrary.wiley.com/doi/
       abs/10.1002/joc.1912, 2010.

Samuels, R., Hochman, A., Baharad, A., Givati, A., Levi, Y., Yosef, Y., Saaroni, H., Ziv, B., Harpaz, T., and Alpert, P.: Evaluation and
       projection of extreme precipitation indices in the Eastern Mediterranean based on CMIP5 multi-model ensemble, International Journal of
       Climatology, 38, 2280–2297, https://doi.org/10.1002/joc.5334, https://rmets.onlinelibrary.wiley.com/doi/abs/10.1002/joc.5334, 2018.

350 Scoccimarro, E., Gualdi, S., Bellucci, A., Zampieri, M., and Navarra, A.: Heavy precipitation events over the Euro-Mediterranean region in a
       warmer climate: results from CMIP5 models, Regional Environmental Change, 16, 595–602, https://doi.org/10.1007/s10113-014-0712-y,
       https://doi.org/10.1007/s10113-014-0712-y, 2016.

Seager, R., Liu, H., Henderson, N., Simpson, I., Kelley, C., Shaw, T., Kushnir, Y., and Ting, M.: Causes of Increasing Aridification of the
       Mediterranean Region in Response to Rising Greenhouse Gases, Journal of Climate, 27, 4655–4676, https://doi.org/10.1175/JCLI-D-13-
355   00446.1, https://doi.org/10.1175/JCLI-D-13-00446.1, 2014.

Seidel, D. J., Fu, Q., Randel, W. J., and Reichler, T. J.: Widening of the tropical belt in a changing climate, Nature Geoscience, 1, 21–24,
       https://doi.org/10.1038/ngeo.2007.38, https://doi.org/10.1038/ngeo.2007.38, 2008.

Sen, P. K.: Estimates of the Regression Coefficient Based on Kendall's Tau, Journal of the American Statistical Association, 63, 1379–1389,
       https://doi.org/10.1080/01621459.1968.10480934, https://www.tandfonline.com/doi/abs/10.1080/01621459.1968.10480934, 1968.

360 Shohami, D., Dayan, U., and Morin, E.: Warming and drying of the eastern Mediterranean: Additional evidence from trend analysis, Journal
       of Geophysical Research: Atmospheres, 116, https://doi.org/10.1029/2011JD016004, https://agupubs.onlinelibrary.wiley.com/doi/abs/10.
       1029/2011JD016004, 2011.

Stott, P. A., Stone, D. A., and Allen, M. R.: Human contribution to the European heatwave of 2003, Nature, 432, 610–614,
       https://doi.org/10.1038/nature03089, 2004.

365 Totz, S., Petri, S., Lehmann, J., and Coumou, D.: Regional Changes in the Mean Position and Variability of the Tropical Edge, Geophysical
       Research Letters, 45, 12,076–12,084, https://doi.org/10.1029/2018GL079911, https://agupubs.onlinelibrary.wiley.com/doi/abs/10.1029/
       2018GL079911, 2018.

Wang, B., Liu, J., Kim, H.-J., Webster, P. J., and Yim, S.-Y.: Recent change of the global monsoon precipitation (1979–2008), Climate
       Dynamics, 39, 1123–1135, https://doi.org/10.1007/s00382-011-1266-z, https://doi.org/10.1007/s00382-011-1266-z, 2012.

370 Zampieri, M., Ceglar, A., Dentener, F., and Toreti, A.: Wheat yield loss attributable to heat waves, drought and water excess at the global,
       national and subnational scales, Environmental Research Letters, 12, 064 008, https://doi.org/10.1088/1748-9326/aa723b, https://doi.org/
       10.1088%2F1748-9326%2Faa723b, 2017.

Zappa, G., Hawcroft, M. K., Shaffrey, L., Black, E., and Brayshaw, D. J.: Extratropical cyclones and the projected decline of win-
       ter Mediterranean precipitation in the CMIP5 models, Climate Dynamics, 45, 1727–1738, https://doi.org/10.1007/s00382-014-2426-8,
375   https://doi.org/10.1007/s00382-014-2426-8, 2015.

Zscheischler, J. and Seneviratne, S. I.: Dependence of drivers affects risks associated with compound events, Science Advances, 3, https://doi.org/10.1126/sciadv.1700263, https://advances.sciencemag.org/content/3/6/e1700263, 2017.

Zscheischler, J., Westra, S., van den Hurk, B., Seneviratne, S., Ward, P., Pitman, A., AghaKouchak, A., Bresch, D., Leonard, M., Wahl, T., and Zhang, X.: Future climate risk from compound events, Nature Climate Change, 8, 469–477, https://doi.org/10.1038/s41558-018-0156-3, 2018.

380